WMO/CAS/WWW

EIGHTH INTERNATIONAL WORKSHOP ON TROPICAL CYCLONES

8.2: Challenges and Advances related to TC Rainfall Forecast

Rapporteur: WOO Wang-chun
Hong Kong Observatory
134A Nathan Road, Tsim Sha Tsui, Kowloon, Hong Kong, China.

Email: wcwoo@hko.gov.hk
Phone: +852 2926 8453

Working group: (*by surnames in alphabetical order)*

Wallace HOGSETT	Weather Analytics, Inc. (previously National Oceanic and Atmospheric Administration)
M. MOHAPATRA	Indian Meteorological Department
Kazuhiko NAGATA	Japan Meteorological Agency
Peter OTTO	Bureau of Meteorology, Australia
QI Liangbo	Shanghai Meteorological Bureau, China Meteorological Administration
VO Van Hoa	National Hydro-Meteorological Service, Viet Nam
XU Yinglong	China Meteorological Administration

Abstract:

Precipitation from tropical cyclones (TC) immensely affects the livelihood of people across the globe. While playing an important role to water supplies, TC rain that comes too intensely and rapidly can claim many lives and cause substantial damage to infrastructure through flooding, landslides and other secondary disasters. An effective warning system supported by sound science, observation networks, forecast support systems and warning message dissemination procedures is necessary to mitigate such adverse impacts.

This report starts with progresses made to the observation network as well as methods to compute Quantitative Precipitation Estimate (QPE) and Quantitative Precipitation Forecast (QPF) in several National Meteorological and Hydrological Services (NMHS). Generally speaking, observation networks and forecast systems have significantly advanced in the past four years. It however remains a challenge to forecast and warn for severe weather in a timely, accurate and precise manner. Some limitations, such as relatively sparse maritime observations, would be hard to overcome but still a lot of improvements, like enhancing QPE algorithms, advection-based models, and NWP models, could be achievable. The report concludes with a number of recommendations for NMHS to consider when formulating strategies to meet challenges in forecasting TC rainfall.

8.2.0. Introduction

Globally, 80 to 100 TCs develop over tropical oceans every year (UKMO 2014). For each country on the rim of the western North Pacific and the South China Sea, the most active TC basin, there are often several TCs making landfall per year. Even in less active basins, it is not uncommon for a country to experience a significant TC impact once every couple of years.

TCs always bring rain to places along their path and often result in intense precipitation, significant landslides and severe flooding, leading to the loss of life, infrastructure damage and a multitude of consequential hazards such as tree failures and traffic accidents. Along with dangerous winds and storm surges, heavy rainfall is one of the most deadly causes of a TC. Urbanization and climate change add further complexity to the issue.

Potential dangers aside, it is worth noting that TC rainfall is also crucial to water supplies and agriculture. The contribution of TC rainfall to the global precipitation is discussed in Jiang & Zipser (2014). As an example, TC rainfall accounts for about a quarter of the annual rainfall of southern China. The hydrological system is therefore affected in both ways; too much TC rainfall causes flooding while too little TC rainfall results in droughts. A greater understanding of TC rainfall possibilities is therefore required to improve the livelihood of the population.

Weather warnings are only as good as observations allow. QPE not only enables us to understand what is happening but also provides essential data for verification. Over the past few years there have been significant improvements in the observation networks in many countries due to the launch of satellites fitted with fast and high resolution sensors, the installation of new radars, an increased in the density of rain gauge networks, as well as enhancements to processing and quality control software. It however remains a challenge for many places, particularly those in less developed countries, to secure the resources necessary for maintaining, updating and expanding the observation networks. Data remains sparse over the ocean, yet this is a vast area where TCs spend most of their lives. Nevertheless, advances in technology open up the possibility to collect better observation data in a more affordable manner (e.g. the proliferation of wireless networks for data telemetry and the emergence of unmanned aerial vehicles). To further build up capacity against adverse impacts from natural disasters, continuous investments in conventional instruments, the innovative use of remote sensing technology, and further technological developments are required.

There is an ever increasing demand for more accurate and precise QPF, along with longer lead times for threshold crossing events. While striving to satisfy these needs, it is worth remembering that a warning earns its reputation by sticking to the science and evolving through constant verification. Products with low skill, no matter how high their resolution are, may therefore not be suitable for public consumption. Furthermore, the inherent uncertainties should ideally be communicated, and a range of scenarios may be provided to users trained to interpret them. For instance, hydrologists increasingly require not only a single-figured catchment averages but several figures within the catchment complete with confidence levels.

A number of forecast systems are in place to cope with rainfall in TC scenarios. Some of them are dedicated solely to TC rainfall, such as the “Ensemble Tropical Cyclone Rainfall Potential (eTRaP)” by National Oceanic and Atmospheric Administration (NOAA), while some others are more general and function irrespective of the rainfall type. A number of general rainfall forecast systems have incorporated TC rainfal specific modules, such as the TC module for the “Short-range Warning of Intense Rainstorms in Localized System (SWIRLS)” by the Hong Kong Observatory (HKO).

8.2.1. Progresses in the Past 4 Years

8.2.1.1 Observations

There were notable enhancements to the observation networks in the past 4 years. New satellites capable of rapid scanning were launched. Additional radar stations were also established in many countries, and the density of rain gauge networks were significantly increased in numerous developing countries.

The China Meteorological Administration (CMA) launched the geostationary satellite Fengyun-2F (FY-2F) in 2012 and since then intense observations have been made whenever a TC was expected to affect the Chinese coast. When the intense observation mode is activated, a satellite image is taken every 6 minutes, providing forecasters with an immensely useful tool to monitor the development and evolution of TC rain bands.

The Indian Meteorological Department (IMD) operates a dense network of rain recording stations which are being used in synoptic forecasting, hydro-meteorological applications like flash flood forecasting and in NWP models. There are 552 synoptic observation stations, 2868 daily rainfall monitoring sites and 675 automatic weather stations (AWS). In addition to the 1,300 rain gauges maintained by IMD, state governments maintain over 3,540 rain gauges, and the data from these instruments is made available to the IMD in manuscript form through the Railways, Forest and Agriculture Departments and other organisations which maintain about 5,039 non-reporting rain gauge stations to meet their specific needs. IMD has planned to establish a network of about 1,000 AWS and 5,000 Automatic Rain gauge stations in phased manner.

In March 2014, the Japan Meteorological Agency (JMA) increased the resolution of its radar images from 1 km to 250 m through upgrading the processing system to obtain a more detailed echo distribution.

In Viet Nam, the observation network was significantly expanded over the past 4 years. More than 20 AWS and 150 rain gauges were installed across the nation. In addition, two radiosonde and two Doppler weather radar stations were also put into operation.

In Hong Kong, the HKO and the Hong Kong Polytechnic University jointly established the Community Weather Information Network (Co-WIN). The Co-WIN initiative consists of 130 members, most of which are primary schools, secondary schools, and tertiary institutes. The members participate through the exchange of real-time data gathered via local weather stations. The collected meteorological data is also available via a publicly accessible website. The project has enhanced the HKO's monitoring capability at a minimal cost, and has also provided students of the participating schools/institutes with invaluable opportunities to learn meteorology and gain experience in operating meteorological instruments.

8.2.1.2 Quantitative Precipitation Estimation

Whilst model output is a crucial element of the final forecast, ensuring the veracity of incoming data is also extremely important for any event.

In June 2014, after two years of testing, the CMA's quantitative precipitation estimation (QPE) system ingesting multiple data sources went into operation. The system has fully integrated various QPE products of CMA's Doppler radar network, FY-2/3 series geostationary and polar orbit satellites, and over 40,000 meteorological and hydrological rain gauges. The system now provides real time QPE products with 10 km horizontal resolution every hour (Figure 21).

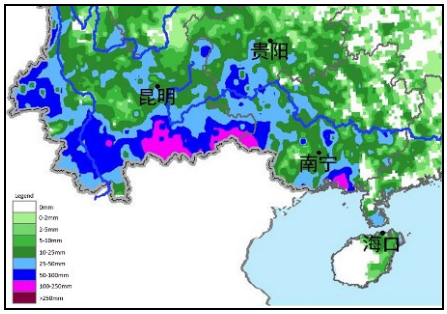

Figure 1. The 24-h precipitation estimation of Super Typhoon Rammasun from 00UTC July 20 to 00UTC July 21 2014, as an operational product in CMA.

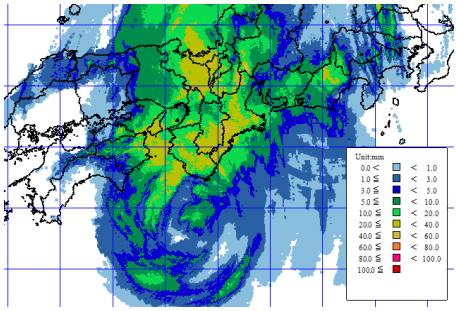

Figure 2. An example of R/A used in JMA: 17 UTC 15 Sep. 2013 (Typhoon MAN-YI)

The JMA produced a QPE product known as Radar/Raingauge-Analyzed Precipitation (hereinafter "R/A"), which shows one-hour cumulative rainfall with a spatial resolution of 1 km, and is updated every 30 minutes (Figure 2). The quality control process was improved with a better noise reduction algorithm to remove echoes aloft taking into account multiple radar data at the same place, and to eliminate bright bands through identifying melting layers from numerical weather prediction (NWP) model outputs.

In Bureau of Meteorology (BoM), Australia, satellite derived rainfall estimates from the Tropical Rainfall Measuring Mission (TRMM) Multi-satellite Precipitation Analysis (TMPA) 3B42 program were compared to gauge-based gridded rainfall analyses over Australia and also over Pacific Ocean atolls and coastal sites. Atoll sites are used as a proxy for "open ocean" sites. The guidance was shown to have good correspondence over space and time with observed rainfall over Australia, with a high correlation coefficient and good skill scores in most cases, though tended to overestimate TC rain for low rain rate events and underestimate TC rain at higher rain rates. Similarly TRMM 3B42 was found to have good skill in detecting intense TC rainfall over the Pacific Ocean (good correlation and pattern matching with the gridded gauge reanalysis), though with some notable deficiencies. Although TRMM 3B42 tended to overestimate heavy rain frequency on atoll sites, its intensity estimates for TC heavy rain over the ocean were nonetheless more skillful than those over land. In particular heavy TC rainfall was significantly underestimated by TRMM 3B42 on coastal and island sites with high elevations, suggesting the estimation method is unable to account for orographic enhancement during the landfall of a TC, a deficiency also noted in the IWTC-VII report. Rainfall intensity estimates derived from polar-orbiting platforms also suffer from coverage limitations when combined within an ensemble (eTRaP), though National Environmental Satellite, Data, and Information Service (NESDIS) is working on a version which derives "HydroEstimator" (infra-red) based rainfall estimates from geostationary satellites, and the output has been found to be only marginally less accurate than the microwave-based output, and is available hourly (Ebert, personal).

In IMD, QPE is calculated as area weighted average rainfall over a river catchment or sub-catchment based on past 24 hour accumulative rainfall. Based on INSAT 3D, three different products, viz, the QPE, INSAT multispectral rainfall estimate and hydrometer estimates are generated in real time every half hourly, daily, monthly and seasonal basis. An example in association with a monsoon depression over eastern India on 21 July 2014 is shown in Figure 3.

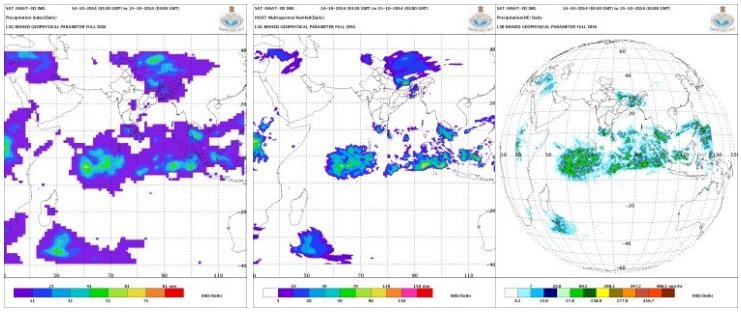

Figure 3. An example of satellite based QPE product in association with a monsoon depression over eastern India

Satya et al. (2012) evaluated the performance of satellite-retrieved precipitation estimation during cyclonic events in the North Indian Ocean. Qualitative and quantitative evaluation of surface rain rates from three different data products, namely TMI-2A12, TMPA-3B42, and GSMaP, were carried out with respect to PR-2A25 data product. The TMPA-3B42 product showed better performance than the other two precipitation products during low to moderate rainfall regimes and the GSMaP precipitation product showed better compliance than the TMPA-3B42 product with PR rain rate under extreme (more than 10 mm/hour) rain events.

IMD has also developed a new high spatial resolution (0.25° × 0.25°) long period (1901-2010) daily gridded rainfall data set over India Region (Pai *et al.* 2014) and daily IMD-NCMRWF (merged SAT + Gauges) rainfall dataset which includes land and north Indian oceanic regions (Mitra *et al.* 2009). Mitra *et al.* (2009) has developed a new technique to estimate rainfall at very fine scale (hourly rain rate at 0.05° × 0.05° spatial resolution) over India and the associated oceanic regions (20° S-40° N, 40° E-130° E). By using infrared (IR) and 6.7-µm water vapour (WV) channel observations from Meteosat-7, a new rain index (RI) is computed. The index computation is composed of two steps. First, the IR and WV brightness temperatures are divided by their respective non-rainy thresholds to get the IR and WV rain coefficients. The product of these coefficients is defined as the RI. These RIs are collocated against rainfall from the precipitation radar on board the TRMM to develop a relationship between the index and the rain rate. The present technique shows a correlation coefficient of 0.74, a bias of 0.086 mm, and a root-mean-square error of 4.78 mm when compared with rain gauge. An example of this product is shown in Figure 4.

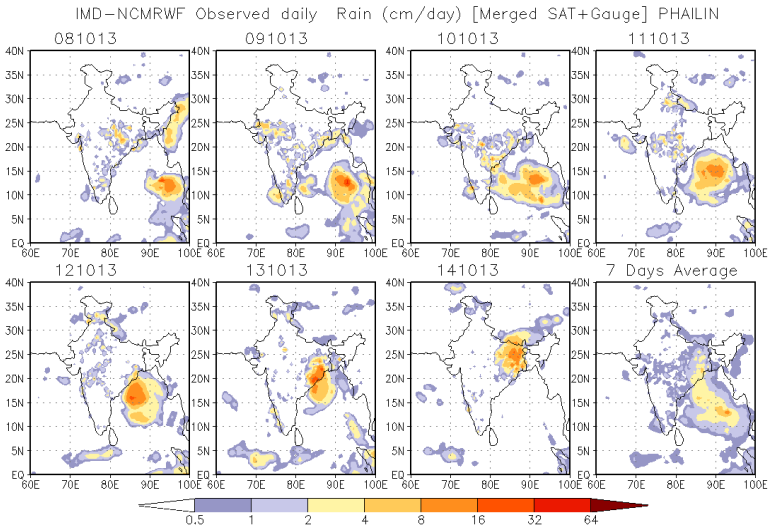

Figure 4. Raingauge and satellite based merged rainfall analysis during TC Phailin period (8-14 October 2013)

A project to generate graphical / pictorial outputs of (i) percentage frequency of rain rate (ii) azimuthally averaged radial profile of rain rate and (iii) quadrant-wise mean rain rate around 43 Tropical Cyclones that affected North Indian Ocean during 2000-2010 using 3-hourly 3B42 TRMM rainfall data is presently being undertaken in the Cyclone Warning Research Center (CWRC) in Chennai, India. Computations are carried out for each cyclone based on intensity stratification (5 stages of intensity are defined) and the

above products are generated for each stage of each cyclone (Balachandran *et al.* 2014). The products are presented using a menu driven user interface and uploaded to the Regional Meteorological Center (RMC) Chennai website. These products will help researchers understand the rainfall patterns associated with each cyclone over the North Indian Ocean during the recent decade. Analysis of TC rainfall asymmetry based on TRMM 3B42 data in relation to Vertical Wind Shear and TC motion has also been carried out (Balachandran & Geetha *in press*)

In Viet Nam, QPE at the National Hydro-Meteorological Service (NHMS) was significantly improved by an increase in the density of the AWS and rain gauge networks and the use of MTSAT and Doppler weather radar data. These QPE products are now assimilated into hydrological models. There is however still room for improvement as the rain gauge network density is increased and modernized.

The HKO and BoM jointly developed a rainfall data quality-control scheme based on radar-raingauge co-kriging analysis. The important threshold values required in the data quality control of 60-min raingauge rainfall were determined from a detailed analysis of the distributions of rainfall residuals defined as the arithmetic difference and the logarithm of the ratio between a raingauge measurement and its co-kriging estimate. The scheme is in real-time use in Hong Kong (Yeung *et al.* 2014).

8.2.1.3 Quantitative Precipitation Forecast

As the spatial resolution of global and regional dynamical prediction systems continues to increase, the ability of these systems to capture important precipitation processes within TCs also continues to increase. Terrain can be represented more realistically than was possible even five years ago. On the other hand, initial conditions (ICs) remain inadequate to fully capture the initial state of the TC circulation. Satellite data, which holds some promise to improve the representation of the TC ICs, remains underutilized in operational prediction systems. The inclusion of cloudy radiances into operational TC models remains a difficult research issue (Zhang *et al.* 2013). Airborne in-situ and radar observations are increasingly used, when available, to improve the ICs.

In the past five years, the NOAA's Hurricane Forecast Improvement Project (HFIP) made a significant investment to improve many aspects of the TC forecast problem. A focus of HFIP is improving intensity forecast skill, and many of the processes that affect intensification also affect TC rainfall. Significant progress has been made on TC rainfall forecasts through HFIP and the broader research community. For example, Weng & Zhang (2012) used an ensemble Kalman-filter system to assimilate aircraft radar observations into the Weather Research and Forecasting (WRF) model. A technique for assimilating radar observations was first included in NCEP operational TC model forecasts in 2013. Advanced data assimilation techniques are being tested to provide a more accurate initial state (e.g. Cavallo *et al.* 2013).

Higher resolution regional prediction systems, such as the NCEP HWRF and the community WRF, are now able to capture the evolution of TC precipitation at cloud-permitting resolution. Recent studies have shown the ability of high-resolution simulations to capture complex orographic rainfall patterns that are often observed in landfalling TCs (Van Nguyen & Chen 2011). As the resolution and physics of limited-area models increases in operations, the skill of TC rainfall forecasts will continue to improve.

Global prediction systems including the NCEP Global Ensemble Forecast System (GEFS) and the ECMWF ensemble system are increasingly capable of accurately forecasting TC rainfall. Resolution increases, data assimilation advancements, and improved physics are contributing to the improvements. Further, reforecast datasets (Hamill *et al.* 2013) are an emerging tool for precipitation forecasts in general, and they may have some utility to statistically correct TC rainfall forecasts. As reforecasts are adopted by operational forecast centers, skillful corrections to rainfall forecasts may be possible. Other methods to statistically correct ensemble-based TC rainfall forecasts (e.g. Fang & Kuo 2013) also show promise to improve global and

regional TC rainfall forecasts.

Because of the multi-scale interactions and nonlinear character of TC evolution, probabilistic, ensemble-based forecasts can be especially valuable for TC rainfall forecasts. The NCEP Weather Prediction Center (WPC) provides rainfall forecasts for landfalling TCs in the US. WPC forecasters provide not only a deterministic rainfall forecast, but now also a full suite of probabilistic forecasts based on both forecaster input and an objective multi-model ensemble distribution. Users may choose a specific QPF threshold to estimate the likelihood that that the threshold will be exceeded.

In addition, NOAA provides probabilistic, satellite-based precipitation forecasts using the Ensemble Tropical Rainfall Potential (eTRaP) method (Ebert *et al.* 2011). The eTRaP products combine precipitation estimates from multiple satellite sensors to account for uncertainty in the quantitative and spatial aspects of each sensor. Products are available online for all TCs globally.

The National Meteorological Center (NMC) of CMA established a rapid radar data assimilation and nowcasting system for landfalling typhoons since the typhoon season in 2011. Targeted to landfalling typhoons, the system makes use of wind and precipitation retrieved from the updated weather radar network. It incorporates inversed Doppler radar data and other conventional data, including surface and sounding observations, based on 3D-VAR data assimilation and composite cloud analysis technique developed by Oklahoma University. This system has a horizontal resolution with 10 km and runs 8 times per day (00, 03, 06, 09, 12, 15, 18, 21 UTC) and provides guidance for operational TC rainfall forecast and warning. Figure 5 illustrates the 24-hour accumulated precipitation forecast in the case of Super Typhoon Rammasun (2014) from 06 UTC July 18 to 06 UTC July 19 2014.

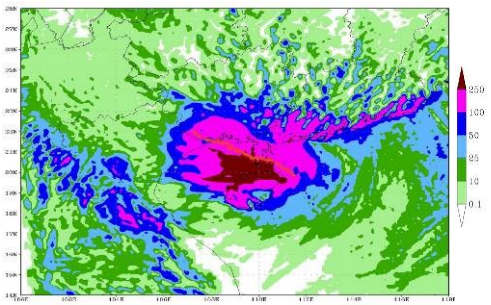

Figure 5. The 24h accumulated precipitation forecast of Rammasun from 06UTC July 18 to 06UTC July 19 2014, as an operational product from a rapid radar data assimilation and nowcasting system for landfalling typhoons of NMC/CMA.

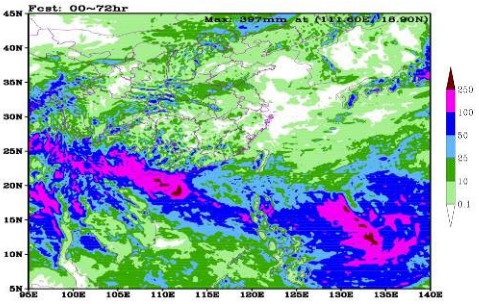

Figure 6. The 72h accumulated precipitation forecast of NMC/CMA GRAPES-TYM for Rammasun (2014).

NMC/CMA's Global/Regional Assimilation Prediction System (GRAPES) Regional Typhoon Prediction Model (GRAPES-TYM) became operational in the 2011 typhoon season, and has since provided guidance on operational fine wind and precipitation forecasting. This model was developed based on CMA GRAPES-MESO model with 15 km horizontal resolution and provides 72-hour track, intensity, wind and precipitation forecast products (Figure 6). Some improvements in GRAPES-TYM had been made in TC vortex initialization scheme, physical process and dynamic framework. The vortex initialization scheme uses the artificial vortex technique based on the nonlinear equilibrium model and combines with Geophysical Fluid Dynamics Laboratory (GFDL) TC separation technique. The improvements in physical process and dynamic framework include improved surface heat flux calculation by correcting surface roughness parameter under strong wind conditions, improved model TC intensity prediction by introducing heat expansion from continuous equation, and adjustment of physical values in the model by introducing surface pressure from TC vortex initialization scheme. Since 2014, the valid forecast time has been upgraded to 120h. Under the CMA NWP project, GRAPES-TYM horizontal resolution will be upgraded to 10, 3-5 km in 2015, 2016 respectively. And it will be a coupled ocean-atmosphere model in 2016.

In 2013, NMC/CMA further developed a 24-hour precipitation grade grid forecast guidance product based on historical ECMWF and T639L60 deterministic forecast products, ingredients method and logistic regression model. The forecast guidance product provides 6-hourly precipitation forecast graded at 13, 25 and 60 mm and 24-hourly precipitation forecast graded at 25, 50 and 100 mm (Figure 7 and Figure 8).

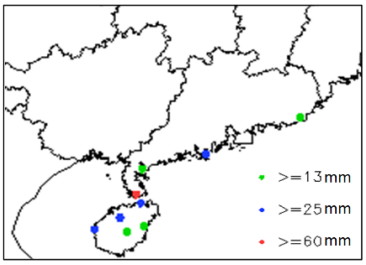

Figure 7. The 6-h precipitation grade forecast of Rammasun from 06UTC July 18 to 12UTC July 18 2014 of NMC/CMA.

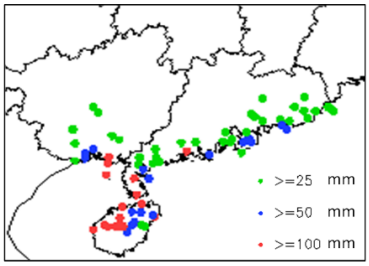

Figure 8. The 24-h precipitation grade forecast of Rammasun from 00UTC July 18 to 00UTC July 19 2014 of NMC/CMA.

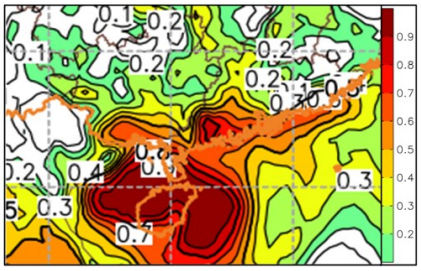

Figure 9. The 24-h extreme precipitation index forecast of Super Typhoon Rammasun (2014) as used by NMC/CMA.

In the same year, a front-end ensemble collection products display analysis platform, named "CMA Ensemble Prediction Toolbox (CEPT)" was developed. CEPT is a human-computer interaction system and incorporates all ensemble products from EPS of CMA, ECMWF, NCEP and Canadian Meteorological Centre (CMC). It provides the ensemble rainfall forecast product such as stamp, mean, dispersion, matching mean probability, median, maximum, minimum and probability percentage of accumulated precipitation related to TCs. In order to further improve the skill of the extreme rainfall related to TCs, NMC/CMA also developed the operational guidance product for the extreme TC rainfall based on the extreme forecast index (EFI) product from ECMWF in July 2013. This product is useful for the improvement in the forecast of the TCs' extreme rainfall distribution area (Figure 9).

The HKO developed an "Analog Forecast System (AFS)" to search for historical cases with weather patterns that are analogous to the current pattern as portrayed by NWP. The method overcomes the inability of global NWP models to forecast mesoscale precipitation (Chan, Fong & Chan 2014).

For advection-based nowcasting, the HKO developed a TC module for the SWIRLS nowcasting system, which separates the motion of the spiraling rain bands from the overall movement of tropical cyclone. The module was back-tested with historical cases in the past ten years, revealing that the new scheme is more capable of preserving tropical cyclone rain band structures and can enhance forecast skillsFigure 10).

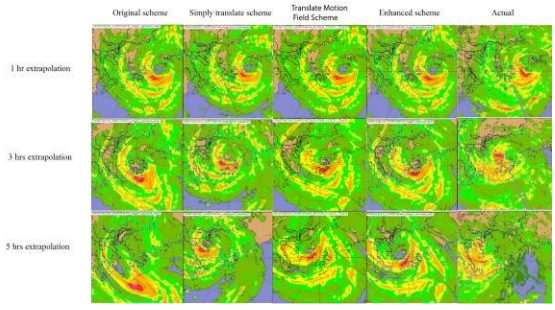

Figure 10. Rainbands of Molave (2009) forecast by SWIRLS. The TC module is more capable of preserving the rain band structure than the original scheme. (Woo, Li & Bala 2014)

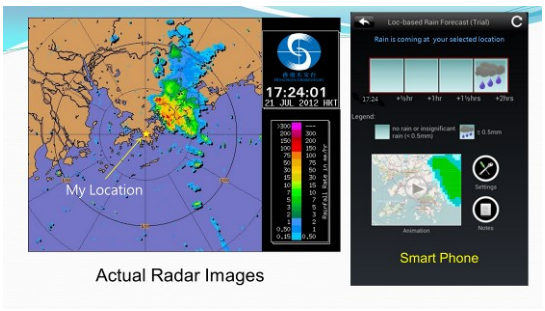

Figure 11. A comparison of the radar image with the location specific rainfall nowcast as shown on MyObservatory of HKO.

In SWIRLS, a new radar echo tracking algorithm based on variational optical flow was adopted and a "SWIRLS Ensemble Rainstorm Nowcast (SERN)" system that comprises 36 members adopting various optical

flow parameters was developed and put into operational use (Woo, 2013b). The enhancements apply to rainfall nowcast in general and are not limited to TC rainfall.

The HKO also developed and started operating a location-specific rainfall nowcast service through a smartphone app for iOS and Android, named "MyObservatory" (Woo, 2013a) and (Woo, 2013c). The new service takes advantage of the capability of smartphones to detect locations and utilizes QPF from SWIRLS to provide location-based rainfall nowcast to the public (Figure 11).

In August 2012 the JMA put into operation the "Local Forecast Model (LFM)", which has a horizontal resolution of 2 km (Hara *et. al.* 2013) and provides 9-hour forecasts every hour followed by the "Very-short-range Forecasting of Precipitation (VSRF)" in October 2013. VSRF is calculated by blending QPF from the JMA's "Meso-Scale Model (MSM)", LFM, and the extrapolated composite echo intensity (Nagata, 2010) to provide hourly QPF out to six hours with a spatial resolution of 1 km. The specifications of the analysis and NWP systems are given in JMA (2014a) and JMA (2014b).

VSRF adopts correlation-based movement vectors to extrapolate radar echoes, from a single common movement vector for a precipitation system during the whole forecast period. It was however observed that this would lead to performance issues due to unnatural precipitation distributions for forecasts beyond the first two hours. Consequently in May of 2014 the accuracy of the system was improved by using two movement vectors; one for up to two hours and another for subsequent hours.

As precipitation systems undergo growth and decay over time, ideally nowcasting should be capable of modelling intensity changes. To further enhance forecast accuracy the VSRF incorporates growth and decay due to orographic effects in the extrapolation process. The JMA introduced two other methods to forecast growth and decay. The first one, implemented in March 2013, considers the short-term intensity change of a precipitation system and led to an increase in the accuracy of forecasts of heavy rain areas. The other method takes into account the intensity trend of forecast precipitation from MSM and LFM and applies the forecast change as growth or decay of the system. Implemented in May 2014, the method improved the accuracy beyond the first two hours.

The JMA operates another precipitation nowcasting service called "Precipitation Nowcast". The scheme provides precipitation intensity forecasts up to one hour ahead with a spatial resolution of 1 km every five minutes. However since August 2014 the JMA started issuing a High-Resolution Precipitation Nowcast with a spatial resolution of 250 m. This higher resolution scheme utilizes the JMA radar data and X-band radar data from the Ministry of Land, Infrastructure, Transport and Tourism (both types of radar have a spatial resolution of 250m) (JMA, 2014c).

The JMA developed EPSgrams to evaluate the uncertainty associated with six hourly accumulated rainfall forecasts from their one-week ensemble prediction model. The plots display the largest and smallest values of the ensemble members, along with the third and first quartiles, and the median. This guidance has been provided to members of the Severe Weather Forecasting Demonstration Project in the South Pacific Islands since November 2010 and in Southeast Asia since March 2012.

In India, the IMD uses a well-known technique from the USA (Tropical Rainfall Potential - TRaP) to forecast rainfall 24 hours prior to TC landfall. The scheme provides useful rainfall forecasts, especially for the coastal areas near the leading edge of an approaching storm. A case study for cyclone 'Aila' (Biswas *et al.* (2012)) used satellite derived rain rates to forecast potential tropical cyclone rainfall accumulations. In their study, an attempt was made to estimate 24 hour rainfall over coastal stations before the landfall of tropical Cyclone 'Aila' using TRMM satellite rain rate data and the observed storm track of Aila.

The IMD operationally runs two regional models, WRF and Hurricane WRF (HWRF) for short-range prediction and one Global model T574L64 for medium range prediction (7 days). The WRF-Var model is run at

a horizontal resolution of 27 km, 9 km and 3 km with 38 Eta levels in the vertical and the integration is carried up to 72 hours over three domains covering the area between lat. 25^{o} S to 45^{o} N long 40^{o} E to 120^{o} E. Initial and boundary conditions are obtained from the IMD's Global Forecast System (IMD-GFS) at the resolution of 23 km. The boundary conditions are updated at six hourly intervals. The IMD also makes use of NWP products prepared by some other operational NWP Centres such as the ECMWF (European Centre for Medium Range Weather Forecasting), NCEP, and the JMA. The hurricane WRF (HWRF) model and Ensemble prediction system (EPS) has been implemented at the NWP Division of the IMD HQ for operational forecasting of cyclones. The QPF was also developed based on the GFS and WRF models for different river catchments and sub-catchments. There is also a multi-model ensemble (MME) technique to provide the daily 24 hr accumulative rainfall over each district (smallest geographical area of the country for administrative purpose) and the river catchment. Additionally a 20-member Global Ensemble Forecast System (GEFS) runs at the National Centre for Medium range weather forecasting (NCMRWF) in India, and the scheme provides probabilistic precipitation forecasts for different thresholds of rainfall and EPS grams for specific locations.

The synoptic, statistical and satellite/radar guidance can help short range forecasting (up to 12/24 hrs), while NWP guidance is mainly used for 24-120 hr forecasts. The RSMC's manual input into the short range forecasting is supported by observations, standard operating procedures, check lists, road maps and a digitised decision support system (IMD, 2013). Consensus forecasts that gather all or part of the numerical forecast tracks and utilizes synoptic and statistical guidance are employed to issue official forecasts (Mohapatra *et al.* 2013). As NWP models have limitations in correctly predicting the location and intensity of precipitation, the forecasters keep in mind the biases of the models while utilising them for the final forecasts.

In Viet Nam, QPF nowcasts are prepared based on linear extrapolation of 6-12 hours QPE that incorporates satellite and radar data. In the future, dynamic approach will be implemented using QPE in conjunction with QPF from advection-based system such as HKO's SWIRLS and high-resolution NWP models.

NHMS of Viet Nam references various global deterministic and ensemble NWP models for medium range forecasts. It also operates a Short-Range Ensemble Prediction System (SREPS) for forecasts of 1-3 days. SREPS consists of 20 members by running 4 regional models including HRM, WRF-ARW, WRF-NMM, BoLAM in hydrostatic mode with initial and boundary conditions from 5 global forecasts (GEM, GFS, GME, GSM, NOGAPS). The forecast range is 3 days ahead with every 3 hours output. The models run operationally 4 times a day at 00Z, 06Z, 12Z and 18Z. The resolution is 0.15^{0} x 0.15^{0}, 201 x 161 grid points, 31 levels.

NHMS of Viet Nam also references a Limited-area Ensemble Prediction System (LEPS) that consists of 21 members (by running HRM model with ICs and BCs from 21 members of GEFS) with resolution of 0.2^{0} x 0.2^{0}, 201 x 161 grid points, 31 levels, 3-hour interval output. This system operates 4 times per day (00Z, 06Z, 12Z and 18Z) and forecast 5 days ahead.

In order to diagnose areas of extreme rainfall, forecasters use weather charts (surface and upper-air) along with other observations (i.e. satellite, radar, etc.) to analyze synoptic weather patterns and potential threat areas. Forecasters also refer to NWP products (rainfall, wind, divergence, convergence, vertical velocity, relative vorticity, etc.) and probabilistic products are also utilized.

BoM of Australia has been actively developing other means to enhance its forecasts, such as:

- Very high resolution NWP assimilating radar
- Model on demand capability
- Ensemble prediction (medium range) derived from a single model, i.e. ACCESS Global and Regional Ensemble Prediction System (AGREPS)
- Ensemble prediction (medium range) derived from a "poor-man's ensemble" (PME) of different models
- High resolution (2km) ensemble prediction
- End-to-end flood forecasting systems

The PME scheme is now operational, and testing revealed that it worked well for ex-TC Oswald. An example of the 72-96 hour output for that event is shown in Figure 12. The forecast was derived by combining the Australian ACCESS-G output with the model output from the JMA, NCEP, ECMWF, and CMC. Using a method based on the work of Sloughter *et al.* (2007), the probability distribution of observed rainfall is predicted using the mean ensemble rainfall from the PME. The parameters of the functions used to describe the probability distribution, and its dependence on the ensemble mean rainfall, are fitted using training data from the recent past (35 days prior to the current date, and ± 35 days from the current date in the previous year) (Riley, personal).

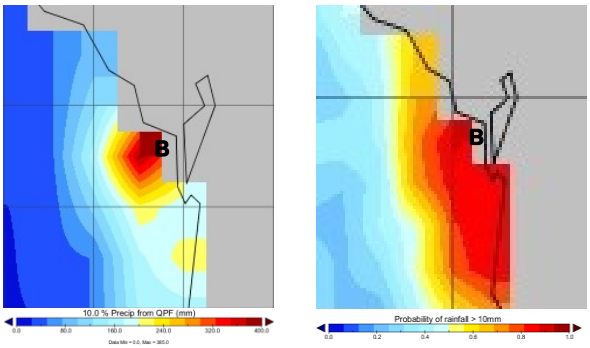

Figure 12. The rainfall amount likely to be exceeded with 10% probability (left) and the probability of > 10 mm rainfall (for 24 hours to 00UTC on 27 Jan; model base 96 hours earlier). Bundaberg is shown by B.

Despite recent technological advances and the very successful medium term forecasts for this and an increasing number of events, the events of ex-TC Oswald show that NWP still does not provide all of the answers, and so there is still an important need to invest in forecaster training. Furthermore, the subjective perceptions of a human are both an asset and at times weakness, yet the mutual development of recommended practice can guide the subjectivity, spread new knowledge across teams, and also give individuals a greater sense of ownership of the process and outcomes.

8.2.1.4 Hydrological Forecast

In India, precipitation inputs, including real time observations and weather forecasts, are used in hydrologic runoff models to generate estimates of rates and stages of stream flow or used in flood prediction models to issue early warning of rainfall-triggered floods. Therefore, hydro-meteorological inputs, generally, and precipitation inputs, specifically, strongly influence real-time hydrologic forecasts. Hydro-meteorological inputs consist of QPEs, QPFs. The accuracy of hydrologic products is largely dependent on the accuracy of QPE and the skill of QPF. Ray (2014) assessed the hydrological aspects of Cyclone Phailin (2013), including the rainfall pattern and flood impact on agriculture.

In Japan, JMA uses the “Soil Water Index (SWI)” and “Runoff Index” for warnings and advisories since May 2008. SWI is calculated up to six hours ahead with a spatial resolution of 5 km, which shows the risk of sediment-related disasters (debris flow, slope failure, etc.) caused by heavy rain. Because the risk becomes higher when the amount of moisture in soil increases, the tank model is used to estimate the amount of moisture in the soil and R/A and VSRF are used as inputs for the tank model. The RI is calculated up to six hours ahead with a spatial resolution of 5 km, and shows the risk of flooding for individual rivers with a length of 15 km or more in the country. In the RI, the tank model is used to estimate outflow, and includes the processes of water flowing down the slopes of the basin (covering an area of about 5 km × 5 km) to the river, and then down the river channel and R/A and VSRF are used as inputs for the model.

At present, NHMS of Viet Nam is using hydrological and hydraulic models to forecast floods and flash floods over most of the major river basins (such as MIKE 11, MIKE 21, NAM, HEC-RAC, MISKINGUM, etc). These models usually use the observed rainfall from the surface observation network (including rain gauges) or from quantitative precipitation estimates based on satellite and weather radar detection, or regional NWP models. The operational hydrological and hydraulic models can be divided into two kinds: (a) a runoff-rainfall

model (requiring the input of data from specific locations such as station observations) and (b) a parameter-distributed model (requiring the input of high-resolution grids). However there are no operational hydrological or hydraulic models to predict landslides or urban inundation.

8.2.2. Notable Case Studies

8.2.2.1 Kompasu (2010) and Lionrock (2010)

Shanghai, China was hit by heavy rain on September 1, 2010, when Typhoon Kompasu (2010) moved to its eastside and Lionrock (2010) to its southern side (Figure 13), a twin TC scenario (Qi and Cao, 2013). The maximum 24-hour accumulated rainfall was 139.5 mm at XuJiahui station with the heavy rain falling in two episodes (Figure 14). For the first episode, the rain band was oriented in north-south direction as a result of the interaction between Kompasu and the cooler air to its west. The second episode, arising from the convergence between the northerly flow over west flank of Kompasu and the moist air from the inverted trough induced by Lionrock, resulted in a rain band oriented primarily in east-west direction (Figure 15). Three operational global models from CMA (T639), ECMWF and JMA were examined and it was found that they all clearly depicted the north-south oriented convergence line and the consequential first episode of rain, though there remained discrepancies in the exact location and the rainfall amount. However, all model runs initialized at 12UTC August 31 failed to capture the second episode. For the ensuing runs, i.e. initialized at 00UTC September 1, the CMA and ECMWF models hinted at the second episode but still failed to capture the significant amount of the rainfall while the JMA model continued to forecast no rainfall at all. Due to the relatively small scale of the rain band, the time and location of the second episode of rain was highly dependent on and thus very sensitive to the relative position, intensity and structure of the two tropical cyclones, which was difficult to be captured well by the global models. A very small displacement of the TC's positions would result in quite different rainfall forecasts.

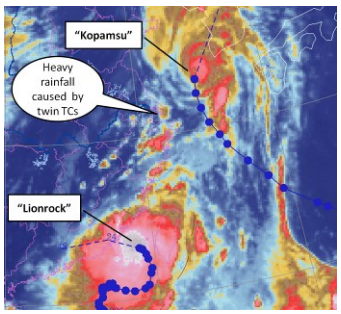

Figure 13. IR cloud image at 09UTC, Aug. 31, 2010

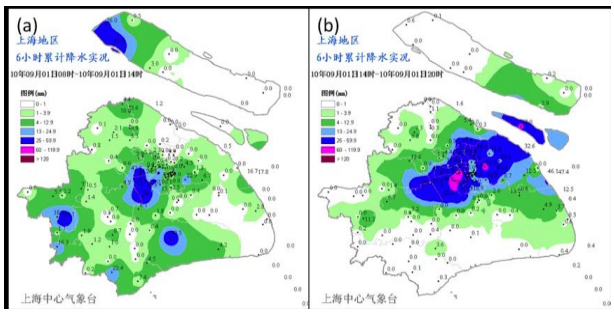

Figure 14. Rainfall in Shanghai during (a) 00 – 06 UTC and (b) 06 – 12 UTC on September 1, 2010 (adapted from Qi and Cao, 2013)

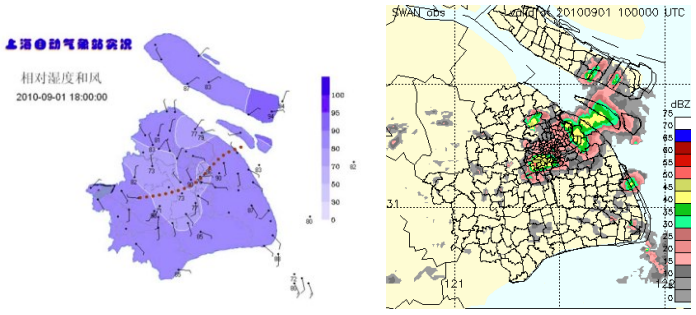

Figure 15. E-W direction convergence line (left) and radar echo band (right) at 10UTC, September 1, 2010 (adapted from Qi and Cao, 2013)

SMB has been operating two sets of the Weather Research and Forecasting (WRF) model since 2008, with resolutions of 15 km and 9 km respectively. The 9 km model (hereinafter "SMB-WRF(9km)")

outperformed the global models by simulating a larger amount of rainfall for the first episode, but still failed to capture the second episode for the run at 12UTC August 31. The run at 00UTC September 1, as shown in Figure 16, forecast a large rain patch correlated with the convergence between the northerly flow from Kompasu and the moist air from Lionrock, though the time and location were off due to the model's small errors in the TC's track, structure and size, critically affecting the convergence zone between the two TCs.

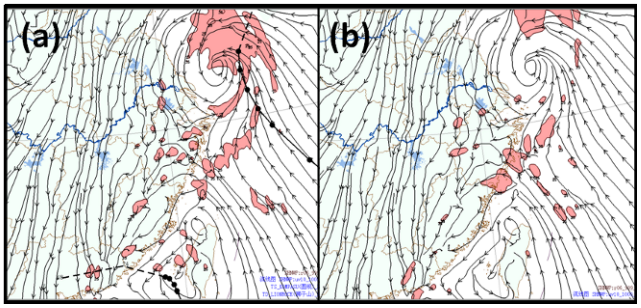

Figure 16. Model outputs from SMB-WRF (9km) for September 1 (Initial time: 00UTC 1 Sep): (a) Stream line of 925hPa at 09UTC and rainfall from 06UTC to 12UTC; (b) Streamline of 925hPa at 15UTC and rainfall from 12UTC to 18UTC. Only rainfall amount over 25mm is contoured. (adapted from Qi and Cao, 2013)

While most of the current operational global models are good at forecasting precipitation brought by synoptic scale features, high resolution regional models have advantages in capturing localized heavy rain. It however remains a challenge for all models, whether global and regional, to provide forecasters with reliable guidance on TC rainfall for cases with multiple TCs.

8.2.2.2 Talas (2011)

As summarized in JMA (2011), Typhoon Talas (2011) formed as a tropical depression over the sea west of the Mariana Islands on 24 August 2011 and then moved slowly northward. It developed into a Typhoon on 30 August. On 3 September, Talas made landfall on Shikoku Island and, after crossing the Shikoku and Chugoku regions, reached the Sea of Japan on the following day. Due to its large scale strong wind area and slow movement, Talas induced moisture advection for many hours and caused the record-breaking heavy rainfall over a wide area from western to northern Japan, especially along the mountains.

Over a wide area of the Kii Peninsula, the total amount of the precipitation from 17 JST (i.e. UTC + 9 hours), 30 August exceeded 1,000 mm. The observing station at Kamikitayama-village in Nara Prefecture observed 1,652.5 mm rainfall in 72 hours, hitting a record high in Japan. The total amount of the precipitation at the station reached 1,805.5 mm, and precipitation in some areas was estimated to be over 2,000 mm based on Radar/Raingauge Analyzed Precipitation. The record-breaking rainfall brought by Talas caused sediment disasters, inundation and river flooding that claimed many around 100 lives, mainly in Wakayama, Nara and Mie Prefectures. In addition, substantial property damage occurred including inundation of homes and rice fields, and damage to railways in a wide area from Hokkaido to Shikoku.

After Talas, JMA introduced a system of Emergency Warnings in August 2013 (JMA, 2013). Emergency Warnings would be issued when a phenomenon is expected to be of a scale that would far exceed the Warning criteria. They are intended for extraordinary phenomena such as Talas, the major tsunami caused by the 2011 Great East Japan Earthquake, in which 18,000 people were killed or left missing, as well as the 1959 storm surge in Ise Bay caused by Typhoon Vera (a.k.a. Ise-wan Typhoon) that claimed over 5,000 lives. Emergency Warnings are disseminated to the public through municipalities and media such as TV and radio in the same way as existing Warnings, Advisories and other bulletins. The issuance of an Emergency Warning for an area indicates a level of exceptional risk of a magnitude observed only once every few decades. Residents are advised to pay attention to their surroundings and relevant information such as municipal evacuation advisories and orders, and should take all steps necessary to protect life.

8.2.2.3 Irene (2011)

Hurricane Irene originated from a tropical wave that moved westward off of Africa and produced a tremendous amount of rainfall as it turned toward the north and moved parallel to the US East Coast (Figure 17). Irene made several landfalls, first in North Carolina and later in New Jersey, just before the center passed directly over New York City. Prior to landfall, forecast impacts of hurricane-force winds and storm surge within the most populous regions along the coast were frequently discussed by the media.

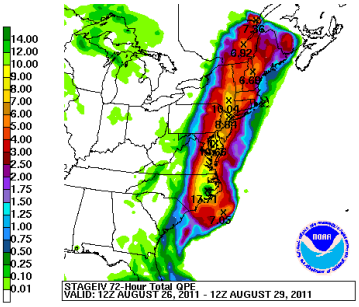

Figure 17. Observed rainfall totals (shaded) from Hurricane Irene (2011). Figure courtesy of the NOAA Weather Prediction Center.

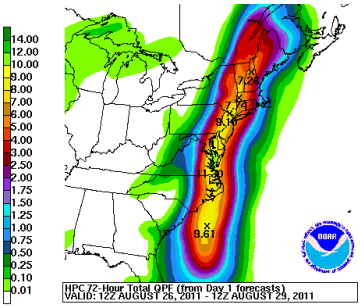

Figure 18. Rainfall forecasts for Hurricane Irene. Three one-day forecasts are combined to create total forecast. Figure courtesy of the NOAA Weather Prediction Center

However, despite the attention that was given to coastal TC hazards, more than half of the 41 deaths in the US were directly attributed to drowning due to rainfall-induced flooding (NHC 2011). In fact, NHC concluded that "Irene's main impact…was rainfall." A subsequent NOAA report on the forecast services during Irene concluded that forecasts for Irene "…did not clearly convey the threat for historic flooding and its associated catastrophic impacts" (NWS 2011). The most devastating flooding occurred in New York, New Jersey and Vermont, where orography and antecedent rainfall likely played a role in enhancing both the rainfall and the subsequent flooding. Rainfall forecasts in advance of Irene were quite skillful (Figure 18), but forecasts for the severity of impacts from the subsequent flooding were not as skillful.

In the time since Irene made landfall, several studies have focused more on understanding the effects of inland TC rainfall. Villarini *et al.* (in press) found that a large portion of the inland US is vulnerable to TC rainfall, emphasizing that TC impacts extend well beyond the immediate coastline. From a science point of view, it is unclear whether the surprise flooding impacts from Irene convey a gap in scientific knowledge or simply a lack of attention. Villarini et al. (in press) noted that inland flooding has received relatively little attention in the literature. On the other hand, the disproportionate number of TC deaths caused by freshwater flooding has been known for some time (Rappaport 2000).

8.2.2.4 Sandy (2012)

Although not technically a TC at the time of landfall, Sandy presented numerous forecast challenges. About a week prior to landfall, the track forecasts from various international ensemble systems showed significant spread. Sandy was forecast to either continue northeastward parallel to the US East Coast, or make a turn to the west and directly impact the Northeast US.

Several days prior to landfall, it became clear that Sandy would indeed turn to the west and impact the USA. The track forecasts from various NWP systems and operational centers converged, and large QPF anomalies were forecast. Interestingly, due to the late-season nature of Sandy, and its interaction with a mid-latitude low-pressure system, not all of the heavy precipitation fell as rain. In fact, nearly 1m of snow fell in some high-elevation locations of the inland US (Figure 19 and Figure 20). Operational forecasters in the US leveraged NWP output to forecast well both the heavy rainfall and the extreme snowfall. The heavy snowfall associated with Sandy, as well as increasing research on "predecessor rain events" (PREs, Bosart *et al.* 2012),

emphasizes that not all TC-related precipitation and impacts occurred in the immediate TC inner core. Sandy was an extreme example of the interaction between a mid-latitude frontal system and a TC, and the dramatic impacts suggest that further research on tropical-extratropical interactions, and the associated impacts, is warranted.

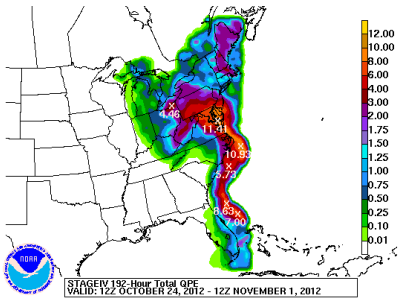

Figure 19. Observed rainfall associated with Sandy. Figures courtesy of the NOAA Weather Prediction Center.

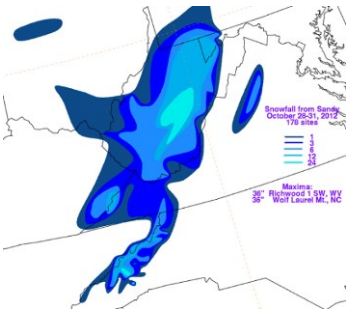

Figure 20. Observed snowfall associated with Sandy. Figures courtesy of the NOAA Weather Prediction Center.

8.2.2.5 Oswald (2013)

Tropical cyclone Oswald crossed the north coast of Australia as a category 1 system[1] late in January of 2013. Despite decaying into a tropical low soon after landfall, the system maintained a strong and broad circulation for over a week as it tracked more than 3,000 km southwards generally near, and inland of Australia's east coast. The rainfall and winds associated with the system produced dangerous ocean swells, storm surges, tornadoes and widespread major flooding over some of the most heavily populated parts of Australia's east coast. Widespread destruction was experienced with USD $2.5 billion of damage incurred to ~6,500 properties across 90 towns across the state of Queensland alone, with six people killed during the week and approximately 40 swift water rescues conducted (Callaghan 2013).

All-time daily rainfall records were exceeded at 26 weather stations, and 1-4 day catchment average records were exceeded within 7 river catchments (Figure 21). Extreme daily totals exceeding 400 mm per day were observed along most of Oswald's track south, though some of the highest of these falls were recorded at two sites inland from Rockhampton (both over 550 mm/day) and two sites in the Gold Coast hinterland (both over 700 mm/day). Trajectory analysis has demonstrated that some of these more extreme rainfall values may be in part attributable to an intensification of Oswald's mid-level circulation after receiving an injection of high PV air descending out of an amplifying upper-level Rossby Wave (Davidson, personal).

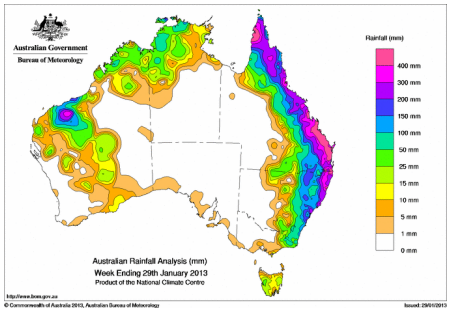

Figure 21. Rainfall analysis (mm) over Australia for the week ending on 29 Jan 2013

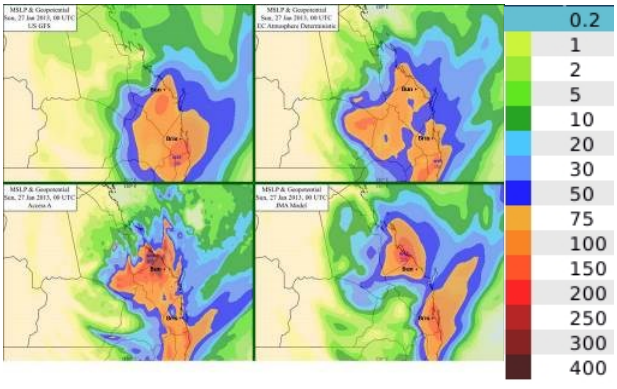

Figure 22. Deterministic NWP output for the 24 hours to 00 UTC on the 27 Jan 2013 (from 12 UTC runs on 25 Jan). The cities of Brisbane (Bris) and Bundaberg (Bun) are also shown.

Deterministic modelling depicted a wide range of possible tracks for Oswald in its formative stages

[1] According to the Australian definition, which is a tropical system with maximum (10-minute) mean winds ≥ 34 knots near the centre, extending more than 50% around the centre, and persisting for at least 6 hours.

north of Australia, however the forecasts converged as the system broadened during its more destructive passage southwards over land, and so track forecasting was generally accurate (error mostly < 100 km) as the system posed its greatest threat to the community. Such consistency was also broadly depicted in the rainfall fields of the deterministic models (Figure 22), and in the local (AGREPS) and ECMWF ensembles over lead times as long as 4-days (Figure 23; Roff, Smith, Naughton and Sulaiman, personal).

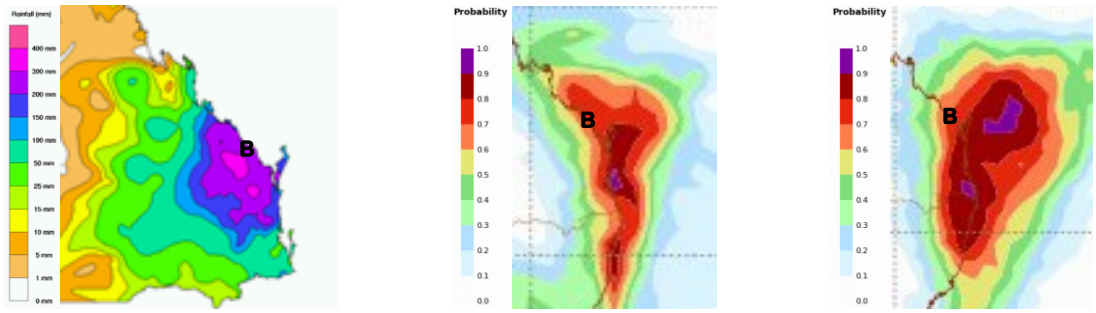

Observed AGREPS-G (+96hrs) ECMWF (+96hrs)

Figure 23. Observed 24-hr totals up to 23UTC on 26th January, and AGREPS-G and ECMWF +96 hour forecast probabilities of ≥ 25mm for an almost equivalent time span (the 24hours up to 00UTC on 27th January). Bundaberg is also shown (B).

The reliability of the guidance and the forecaster's environmental analysis allowed sufficient time for warnings to be issued and for most, yet not all, evacuations to be ordered. Despite the mandatory pre-emptive evacuation of the homes of over 7,000 people along Oswald's path, some residents still found themselves in great danger from extreme falls. Indeed within the Burnett catchment the 1-day catchment average exceeded the previous record by nearly 70%, resulting in a flood peak that broke previous records by several metres at some locations around and within the regional city of Bundaberg (BoM 2013). Over 1000 people had to be rescued by helicopters from rooftops in north Bundaberg as water flowing up to an estimated speed of 70 km/hour damaged and completely washed away structures in the largest such rescue in Australia's history (Callaghan 2013).

The dramatic events at Bundaberg illustrate the high sensitivity to rainfall intensity and distribution inherent within QPF forecasting. Whilst the timing and general nature of the severe rainfall was very well depicted by all deterministic models and ensembles on the *synoptic scale*, the observed falls at many points within Bundaberg's Burnett River catchment were at least double those depicted by most of those models due to widespread *convective scale* rain, resulting in a vastly higher run-off volume. Furthermore the intense convective falls were actually experienced at the more heavily populated lower reaches of the catchment, leaving only ~6 hours of notice for the rooftop evacuations in the city of Bundaberg.

Whilst it remains difficult to reliably model areas of extreme convection, the Brisbane forecasting office has developed techniques to define a threat area where such activity is more likely based upon its synoptic drivers. The definition of the threat area then allows the forecaster to more efficiently focus on monitoring and nowcasting, and also helps them further define the upper limits of rainfall. To define the threat area the forecasters assess a range of model fields from a number of deterministic models (including convergence and precipitable water), and also examine a thermal advection diagnostic that has been successfully used within the office for well over ten years (described in the IWTC VII report; Bonell & Callaghan 2008). The diagnostic is based on the association between warm air advection and isentropic ascent, which in a suitable thermodynamic environment can trigger broad-scale outbreaks of deep convection; outbreaks that can only be broadly approximated via parameterisation within most of the operational models available to forecasters. The technique has subsequently been refined by Tory (2014), who re-derived the thermal advection diagnostic assuming gradient wind balance. An example of the re-derived diagnostic (which we suggest be called the "Callaghan Convection Parameter") for ex-TC Oswald

depicts an area of strong ascent near Bundaberg (YBUD), and a corresponding RADAR image shows the consistency of the threat area with the deep convection at that time (Figure 24).

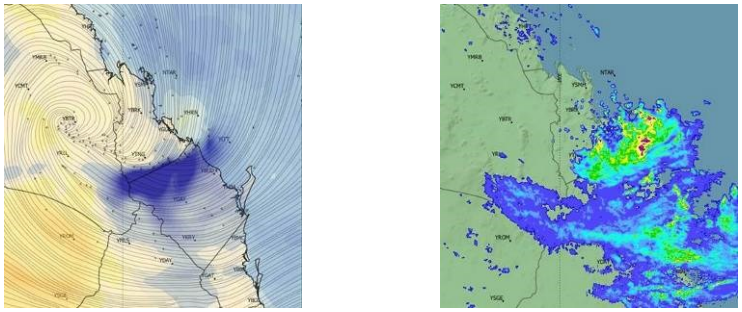

Figure 24. Callaghan Convection Parameter (left) and Composite PPI RADAR image for 00UTC, 26th January 2013 (right)

The only deterministic operational model able to simulate these substantially higher, more localised extremes was the Bureau of Meteorology (BoM)'s Australian Community Climate and Earth-System Simulator (ACCESS)-A model (12 km resolution). For example for the 24 hours leading up to 00 UTC on the 27th of January the Access-A 24-hour rainfall forecast for the Bundaberg region broadly ranged from 200-400 mm/day (with local falls over 800 mm/day), whereas the regional average in the same area on the global models was only 100-200 mm/day (with local maxima of ~175 mm/day in the Bundaberg region). The observations for the same period showed widespread falls consistent with the Access-A output, and three sites in the region reported falls of over 450 mm/day (BoM 2013). Consequently the QPF forecasting was built upon the foundations offered by a good (synoptic-scale) deterministic and ensemble consensus, yet specific catchment average forecast values were ultimately heavily influenced by just one model (Access-A) during the most active days of Oswald's lifespan due to its repeated consistency with observations. Such an informal verification assessment was a crucial means of selecting the guidance for subsequent QPF forecasts, and it is recommended that existing systems be enhanced to provide near real-time rainfall forecast verification (including catchment averages).

Fortunately Access-A's forecast track and synoptic fields were very consistent with the other models throughout the most destructive and dangerous periods of Oswald's passage over land, enabling Access-A to be more heavily relied upon, however such a performance naturally cannot be assumed to be typical.

8.2.2.6 Fitow (2013)

Fitow (2013) formed east of the Philippines late on 30 September 2013. It first moved north-northwestward and gradually intensified into a Severe Typhoon late on 4 October. Then it suddenly turned to move west-northwestward and made landfall in Fujian, China at 17:15 UTC on 6 October, with the maximum sustained wind speed (MSWS) of 42 m/s and the minimum sea level pressure (MSLP) of 955hPa. After landing, Fitow (2013) moved west-southwestward and weakened rapidly (Figure 25).

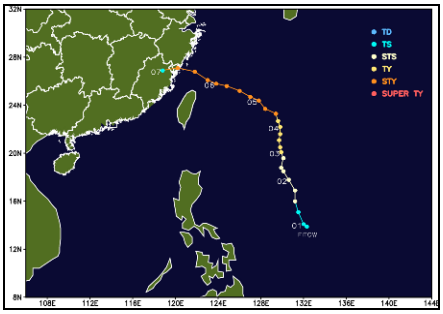

Figure 25. The track of Severe Typhoon Fitow (2013)

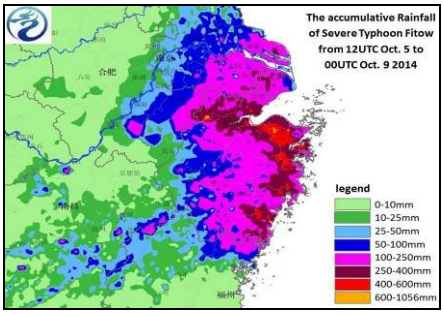

Figure 26. The accumulative precipitation of Fitow from 12UTC 5 Oct to 00UTC 9 Oct, 2013

Fitow was the strongest typhoon made landfall over mainland China except for Taiwan and Hainan islands in October since 1949. The sustained wind speed over Force 13 was recorded over land and extreme gusts over Force 16 were observed over some islands and mountains. The records were broken for both the 10 minutes mean sustained wind speed and gust wind speed.

The interactions of Fitow, cold air and typhoon Danas result in extremely heavy rainfall over eastern China in 6-8 October, with maximum accumulated rainfall reaching 1056 mm. The 24 hour rainfall at several stations was record breaking and the total areas of 24 hour rainfall exceeding 300 mm reached 22,594 km^2 (Figure 26). The extreme rainfall induced by Fitow caused flooding of a rare magnitude in 17 small and medium sized rivers with water levels exceeding the warning lines by 0.09-2.79 m. Some regions in Zhejiang and Shanghai suffered from severe flooding and waterlogging. The city waterlogging lasted almost a week in Yuyao City of Zhejiang Province (Figure 27). A total of 12.16 million people were affected, with 11 dead and 1 missing. The direct economic losses were estimated at RMB 63.14 billion.

Figure 27. The hazards of Fitow in Wenzhou, Zhejiang

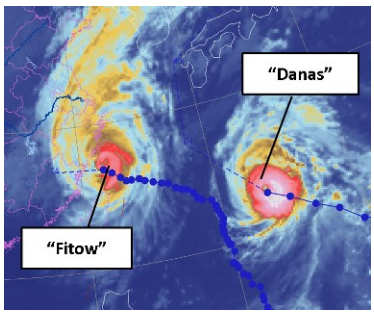

Figure 28. IR cloud image at 12UTC, Oct. 6, 2013

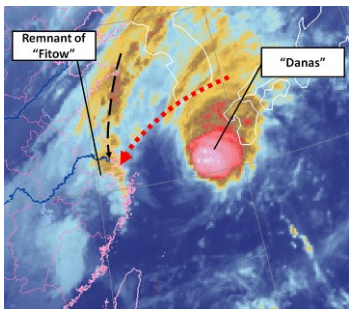

Figure 29. IR cloud image at 18UTC, Oct. 7, 2013.

According to Yu *et al.* (2014), there were two stages with two heavy rain centers during Fitow's landfall: one was near the TC center during 6-7 Oct and the other was related with outer rainfall bands during 7-8 Oct. Shanghai city suffered severely from the rainfall during the second stage, with the level of risk ranking in the top 15% among all TCs that have impacted the Shanghai since 1949. At the time Fitow made landfall, another TC, named Danas, was located to its far east at a distance of about 1,250 km (Figure 28). Cao et al. (2014) suggests that the easterly flow from Danas played an important role in intensifying the precipitation amount in the outer rainband of Fitow after landfall. However, this twin TCs situation differs from that of Kompasu (2010) and Lionrock (2010) (Qi and Cao, 2013) in two ways. Firstly, Fitow and Danas were far away from each other. Secondly, the heavy rainfall in Shanghai occurred in the early morning of Oct. 8, about 24 hours after the landfall of Fitow and with observed precipitation of over 100 mm within 6 hours (Figure 29 and Figure 30(a)). The easterly flow from Danas contributed to a convergence line along with northerly dry flow and supplied abundant water vapour for the heavy rainfall event. The ECMWF global model failed to capture this heavy rainfall event, as it predicted a southwest-northeast oriented rainband (Figure 30(b)) whereas the observed rainband was north-south oriented (Figure 30(a)). SMB-WRF (9 km) captured the convergence line but forecast a too strong easterly flow and a slightly west position of Danas, leading to a forecasted rainband about 50 km west to Shanghai (Figure 30(c)).

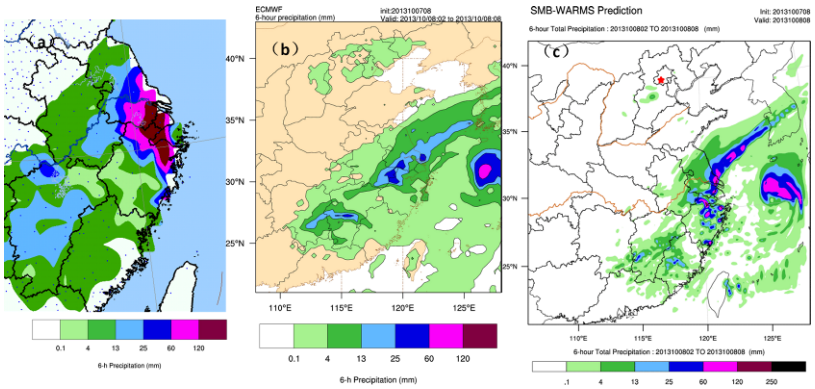

Figure 30. Observed and forecast precipitation from 18UTC 7 to 00UTC 8 Oct, 2013. (a) Observed precipitation; (b) precipitation forecast from ECMWF global model (initial time: 00UTC Oct. 7); (c) precipitation forecast from SMB-WARMS.

8.2.2.7 Phailin (2013)

In October 2013, Phailin formed from a remnant cyclonic circulation which originated in the South China Sea. The circulation remained as a low pressure area (LPA) over the coast of Tenasserim on 6th October 2013, and then a well-marked LPA over north Andaman Sea on 7th October. The LPA deepened into a depression near latitude 12N and longitude 96E, on 8th October. Tracking west-northwestwards, it intensified into a deep depression by 9th morning and further into Cyclonic Storm, named "Phailin" that evening. Moving northwestwards, Phailin further intensified into a Severe Cyclonic Storm in the morning of 10 October and into a Very Severe Cyclonic Storm later that day over the east central region of the Bay of Bengal. Phailin moved northwestwards and crossed the eastern coast of India near Gopalpur (Odisha) around 1700 UTC of 12th October 2013, with a sustained maximum surface wind speed of 215 kph (satellite image depicted at Figure 31). After the landfall, Phailin gradually recurved to north-northwest, then north and finally northeast, as shown in Figure 32.

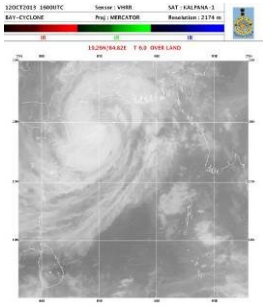

Figure 31. Satellite imagery of Phailin at the time of landfall (1600 UTC of 12 October 2013).

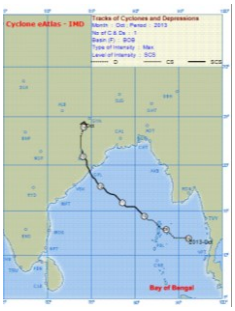

Figure 32. Track of Phailin.

Phailin was the most intense cyclone to cross the Indian coast since the Odisha Super Cyclone of 29th October 1999 (Mohapatra et al, 2002). Phailin underwent rapid intensification from the morning of 10th October to the following morning, with the maximum sustained wind speed increasing from 45 knots to 115 knots. At the time of landfall on 12 October, the maximum sustained surface wind speed was about 115 knots and the estimated central pressure was 940 hPa.

Phailin caused very heavy to extremely heavy rainfall over Odisha resulting in substantial flooding after landfall, the heaviest rain fell over the northeastern sector of the system. The maximum 24 hour cumulative point rainfall was 380 mm in Odisha.

Though model guidance disagreed on the landfall location initially, a consensus eventually emerged as Phailin approached the coast. Indeed the Numerical Weather Prediction (NWP) and dynamical statistical models provided good guidance with respect to Phailin's genesis, track and intensity, however there were spatial and temporal errors in the forecast rainfall.

The IMD accurately predicted the genesis, intensity, track, time and location of landfall, as well as the

quantitative precipitation forecast including the heavy rainfall episodes 4 to 5 days in advance. Proper and timely coordination between the IMD and the crisis management group of the government of India helped in managing the water reservoirs and hence the flooding, thereby minimising the human and economic losses.

Phailin mainly affected the states Odisha and Andhra Pradesh, both along the eastern coast of India. Over 12 million people were affected, of which more than a million had to be evacuated. In Odisha, the cyclone and flooding killed 21 and 17 people respectively. Very heavy to extremely heavy rainfall was recorded over the Andaman & Nicobar Islands, Odisha. Isolated heavy to very heavy rainfall was recorded over adjoining eastern India. The rainfall was higher over north Odisha than over south Odisha. The rainfall extended up to sub-Himalayan West Bengal and Sikkim. Nepal, Bhutan and Bangladesh also received rainfall from this TC, and a maximum 24 hour cumulative rainfall of 38 cm was reported in Odisha.

The rainfall due to Phailin was monitored & predicted continuously since its inception by the IMD/RSMC, New Delhi. At the genesis stage, the rainfall was monitored mainly with satellite observations, supported by meteorological buoys and coastal and island observations. As the system entered into the east central Bay of Bengal, it was mainly monitored by satellite observations supported by buoys. On 12th October, when the system lay within radar range, the Doppler Weather Radar (DWR) at Visakhapatnam was utilized and continuous monitoring by this radar started from 0100 UTC of 12th when the system was at about 310 km east-southeast of Visakhapatnam coast and continued till 1800 UTC of that date. In addition, the observations from satellite, coastal observatories and Automatic Weather Stations (AWS) were used. While coastal surface observations were taken on an hourly basis, the INSAT Kalpana satellite images were sampled every 30-minutes and the DWR radar images every 10-minutes. Satellite images from geostationary satellites Meteosat-7 and MTSAT, along with microwave and high resolution images from polar orbiting satellites (DMSP, NOAA series, TRMM and Metops) were also considered.

The Phailin's rainfall on the 8th October, along with its track, intensity and associated adverse weather (e.g. gales and the storm surge) were predicted exceedingly well and had lead times sufficient to help the disaster managers manage the cyclone in an exemplary manner. Various national and international models and dynamical-statistical models (including the IMD's global and meso-scale models) were utilized to predict the rainfall due to Phailin.

The NCEP HWRF model suggested that the northern parts of the Odisha state would receive heavy to very heavy rainfall (~40 cm) during landfall that was validated by the observations after the event. The IMD also issued an extremely heavy rainfall (25 cm or more in 24 h) warning for 12 and 13 October 2013. Although IMD implemented the 2010 version of the HWRF model for operational TC forecast guidance over the NIO region, the model was run at a reduced resolution (9 km near the storm region). A comparison of the IMD HWRF output with the NCEP HWRF simulation revealed a superior performance from the latter due to its higher resolution, more advanced data assimilation, and advanced model physics (Tallapragada et. al, 2013).

The rainfall forecast issued by the IMD was predicted on Phailin very accurately and well in advance. However, the flood caused by another low pressure area formed over the Bay of Bengal caused extremely heavy rainfall over Odisha during 21-28 October. Due to previous standing water over the region due to TC Phailin the rainfall due to low pressure area caused unprecedented flood over Odisha. As a result the death due to flooding from the low pressure area caused more human deaths and economic losses than the flooding from TC Phailin.

8.2.2.8 Rammasun (2014)

Rammasun (2014) formed east of the Philippines on 12 July 2014. It first moved westward and gradually intensified into a Severe Typhoon, making its first landfall over the southern tip of Luzon in the Philippines with a MSWS of 48ms^{-1} and a MSLP of 945hPa on the 15th of July. Rammasun then crossed southern Luzon and entered the South China Sea while weakening, though it remained a typhoon. On its approach to the northeast coast of Hainan island of China, Rammasun rapidly intensified into a super typhoon with MSWS reaching 60ms^{-1} and MSLP 910hPa right before making a second landfall over Hainan. After this second landing, Rammasun continued to move west-northwestward and successively made its third and fourth landfalls over southern China, with MSWSs of 60ms^{-1} and 48ms^{-1} respectively. It then crossed northern Viet Nam and finally weakened into a tropical depression in Yunnan, China (Figure 33).

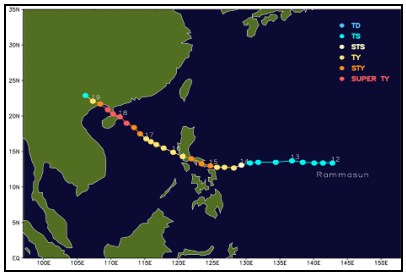

Figure 33. The track of Super Typhoon Rammasun

Figure 34. The hazards of Rammasun in Wenchang, Hainan

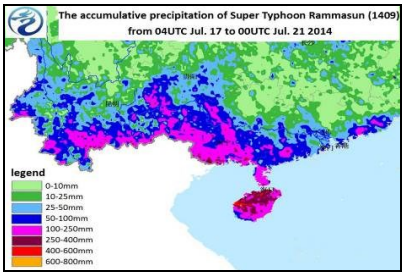

Figure 35. The accumulative precipitation of Rammasun

The maximum intensity of Rammasun was estimated to be 60ms^{-1} in the operational tropical cyclone warning of CMA, making it the strongest typhoon devastating Southern China since 1973 (Figure 34). Sustained wind speeds of over Force 13 were recorded from 04UTC 17 to 00UTC 20, 2014. Gusts over 32.7ms^{-1} lasted up to 6-9 hours. A maximum 10-minute sustained wind speed of 58.7ms^{-1} and a gust of 72.4ms^{-1} were recorded at an island about 100m above sea level, with the MSLP being 899.2hPa. A buoy station over the coastal waters recorded a 10-minute sustained wind speed of 55.1ms^{-1} and a gust of 74.1 ms^{-1}, with the MSLP being 922hPa. So, it is possible that the actual maximum intensity of Rammasun was much higher than the reported 60 ms^{-1}.

Rammasun produced torrential rain over Southern China (Figure 35), with total cumulative rainfalls ranging from 200mm to 500mm. 24-hour rainfalls reached 500mm to 712mm at Hainan Island, with hourly rainfall reaching 100mm to 139mm.

The extreme rainfall induced by Rammasun caused large and rarely seen floods in 13 small and medium sized rivers. The water levels at rivers in Southern China exceeded the warning thresholds, with levels upstream at Nandujiang River in Hainan island breaking the historical record. A total of 11 million people were affected with 62 dead and 21 missing. The direct economic loss was estimated at RMB¥38.48 billion.

Preliminary analyses indicate that Rammasun's rapid intensification and extremely heavy rainfall was caused by the interaction between an abnormally strong upper level jet and cross-equatorial flow. NMC/CMA succeeded in forecasting the rapid intensification of Rammasun over the coastal waters prior to landfall as well as its wind and rain in advance of their impact. The provincial government of Hainan island organized the orderly evacuation of 180,000 people within a 25 km radius of the landfall site, saving lives and minimizing casualties.

8.2.3. Recommendations

While recognizing the progresses achieved in the past few years, it is also realized that the preparation and dissemination of timely, accurate and precise TC rainfall forecasts/warnings remains a challenge given all the limitations ranging from observations to forecast techniques.

This Working Group recommends that NMHS', jointly with academic and research institutes, emergency management agencies and other partner organizations:

- continue to invest in conventional instruments, including further increasing the density of radar and rain gauge networks, and upgrading instruments to increase their accuracy;
- exploring the innovative use of technology to achieve cost-effective enhancements (particularly over maritime environments where observations are relatively sparse) such as improved rainfall schemes derived from the latest rapid-scan satellite imagery and precipitation detection via wireless and public mobile networks;
- continue to develop multi-sensor QPE algorithms that effectively assimilate data from satellites, radars, rain gauges and other instruments;
- continue to improve QPF through the development of high resolution global, regional and limited area NWP models, both deterministic and ensemble, as well as model post-processing techniques and interactive analysis and visualization platforms to meet the needs of operational rainfall forecast and warning services;
- work towards enhancing near real-time model verification with a view to facilitating the selection of the best performing models while an event is still in progress;
- further develop the science behind TC rainfall forecasting, such as identifying data assimilation schemes, cloud physics, dynamical processes, vortex initialization techniques, rainfall catchment climatology etc.;
- develop and follow with appropriate flexibility standard operating procedures;
- expand partnerships with conventional media and explore the use of social networks for clear, concise and timely dissemination of warning messages;
- proactively share and exchange data with other NMHS and partner organizations; and
- engage in capacity building efforts of developing countries through technology transfer and the provision of international training.

8.2.4. Acronyms used in the report:

Acronym	Full
ACCESS	Australian Community Climate and Earth-System Simulator
ADAS	ARPS Data Analysis System
AFS	Analog Forecast System
AGREPS	ACCESS Global and Regional Ensemble Prediction System
ARPS	Advanced Regional Prediction System
BoM	Bureau of Meteorology, Australia
Co-WIN	Community Weather Information Network
CMA	China Meteorological Administration
CMC	Canadian Meteorological Centre
CWRC	Cyclone Warning Research Center
DWR	Doppler Weather Radar

Acronym	Full
eTRaP	Ensemble Tropical Rainfall Potential
EFI	extreme forecast index
GFDL	Geophysical Fluid Dynamics Laboratory
GRAPES	Global/Regional Assimilation Prediction System
HFIP	Hurricane Forecast Improvement Project
HKO	Hong Kong Observatory
IMD	India Meteorological Department
IR	infrared
JMA	Japan Meteorological Agency
LPA	low pressure area
MSLP	mean sea level pressure
MSWS	maximum sustained wind speed
NCEP	National Centers for Environmental Prediction, NOAA
NESDIS	National Environmental Satellite, Data, and Information Service
NHC	National Hurricane Center, NOAA
NHMS	National Hydro-meteorological Service, Viet Nam
NMHS	National Meteorological and Hydrological Services
NMC	National Meteorological Center of CMA
NOAA	National Oceanic and Atmospheric Administration
NWP	Numerical Weather Prediction
NWS	National Weather Service of NOAA
PME	poor-man's ensemble
RI	Rain Index
RMC	Regional Meteorological Center
SMB	Shanghai Meteorological Bureau
SWIRLS	Short-range Warning of Intense Rainstorms in Localized System
TC	tropical cyclone
TMPA	TRMM Multi-satellite Precipitation Analysis
TRMM	Tropical Rainfall Measuring Mission
UKMO	United Kingdom Meteorological Office
USA	The United States of America
WV	Water vapour
WRF	Weather Research and Forecasting
QPE	Quantitative Precipitation Estimate
QPF	Quantitative Precipitation Forecast

8.2.5. References

Abhilash, S., A K Sahai, K. Mohanakumar, John P George, Someshwar Das, 2012: Assimilation of Doppler Weather Radar Radial Velocity and Reflectivity Observations in WRF-3DVAR System for Short-Range Forecasting of Convective Storms, *Pure Appl. Geophys.*, 01⁄2012.

Balachandran, S. & B. Geetha, in press: Characterisation and asymmetry analysis of rainfall distribution associated with Tropical Cyclones over Bay of Bengal: NISHA (2008), LAILA (2010) and JAL(2010), *Mausam*.

Balachandran, S., B. Geetha, K. Ramesh & N. Selvam, 2014: TCRAIN – A database for Tropical Cyclone Rainfall Products for North Indian Ocean, *Tropical Cyclone Research and Review*, 2014, 3(2): 122-129.

Biswas, H. R., P. K. Kundu & D. Pradhan, 2013: A case study for cyclone 'Aila' for forecasting rainfall using satellite derived rain rate data, *Mausam*, 64, pp 77-82.

BoM, 2013: *Special Climate Statement 44 – extreme rainfall and flooding in coastal Queensland and New South Wales*. http://www.bom.gov.au/climate/current/statements/scs44.pdf

Bonell, M. & J. Callaghan, 2008: The synoptic meteorology of high rainfalls and the storm runoff response in the Wet Tropics. *Living in a Dynamic Tropical Forest Lands*, Blackwell Press, 448 pp.

Bosart, L.F., J.M. Cordeira, T. J. Galarneau, B.J. Moore & H.M. Archambault, 2012: An Analysis of Multiple Predecessor Rain Events ahead of Tropical Cyclones Ike and Lowell: 10–15 September 2008. *Mon. Wea. Rev.*, 140, 1081–1107.

Callaghan, J., 2003: Cyclone Oswald Case Study. *Harden Up website*. http://hardenup.org/be-aware/weather-events/events/2010-2019/130120-cyclone-oswald.aspx

Cao, Xiaogang et al., 2014: Impact of twin TC and cold air on '10.8' heavy rainfall event in Shanghai. *Torrential Rain and Disasters (in Chinese, to be published)*.

Cavallo, S.M., R.D. Torn, C. Snyder, C. Davis, W. Wang & J. Done, 2013: Evaluation of the Advanced Hurricane WRF Data Assimilation System for the 2009 Atlantic Hurricane Season. *Mon. Wea. Rev.*, 141, 523–541.

Chan, S.T., C.H. Fong & M.Y. Chan, 2014: An Analog Forecast System for Precipitation Forecasting. *28th Guangdong-Hong Kong-Macao Seminar on Meteorological Science and Technology*, Hong Kong, 13-15 January 2014. http://www.hko.gov.hk/publica/reprint/r1097.pdf

Debnath G.C. & P. Mandal, 2012: The role of orography in producing extremely on the role of orography in producing extremely heavy rainfall induced by cyclonic storm Aila - A WRF model analysis for disaster management. *WMO Technical Document on proceedings of Second International Conference on Indian Ocean Tropical Cyclones and Climate Change (IOTCCC-II)*, New Delhi, 14-17 February 2012.

Ebert, E.E., M. Turk, S.J. Kusselson, J. Yang, M. Seybold, P.R. Keehn & R.J. Kuligowski, 2011: Ensemble Tropical Rainfall Potential (eTRaP) Forecasts. *Weather Forecasting*, 26, 213–224.

Fang, X. & Y.H. Kuo, 2013: Improving Ensemble-Based Quantitative Precipitation Forecasts for Topography-Enhanced Typhoon Heavy Rainfall over Taiwan with a Modified Probability-Matching Technique. *Mon. Wea. Rev.*, 141, 3908–3932.

Haggag Mohammed & Hesham Badry, 2012: Hydrometeorological Modeling Study of Tropical Cyclone Phet in the Arabian Sea in 2010, *Atmospheric and Climate Sciences* Vol. 2, No. 2 (2012), Article ID: 18822, 17 pages. doi:10.4236/acs.2012.22018

Hamill, T. M., G.T. Bates, J.S. Whitaker, D.R. Murray, M. Fiorino, T. J. Galarneau, Y. Zhu & W. Lapenta, 2013: NOAA's Second-Generation Global Medium-Range Ensemble Reforecast Dataset. *Bull. Amer. Meteor. Soc.,* 94, 1553–1565.

Hara, T. *et al*., 2013: The operational convection-permitting regional model at JMA.

IMD, 2013: Cyclone Warning in India: Standard Operation Procedure (2013)

Jiang, H. Y. & E. Zipser, 2014: Contribution of Tropical Cyclones to the Global Precipitation, *3rd International Workshop on Tropical Cyclone Landfall Processes (IWTCLP-III)*, Jeju, 8-10 Dec 2014.

JMA, 2011: Typhoon Talas relevant information -Portal-. http://www.jma.go.jp/jma/en/typhoon_Talas.html

JMA, 2013: FAQ (Emergency Warnings). http://www.jma.go.jp/jma/en/Emergency_Warning/FAQ.html

JMA, 2014a: Specifications of JMA's objective analysis systems. http://www.jma.go.jp/jma/jma-eng/jma-center/nwp/specifications_analysis.pdf

JMA, 2014b: Specifications of the JMA's NWP models and Ensemble Prediction Systems. http://www.jma.go.jp/jma/jma-eng/jma-center/nwp/specifications_models.pdf

JMA, 2014c: High-resolution Precipitation Nowcasts. http://www.jma.go.jp/en/highresorad/

Kumar, N., M. Mohapatra & S. D. Attri, 2014: Landfalling Cyclonic disturbances & climate teleconnections associated with changing rainfall pattern along the east coast of India, *3rd International Workshop on Tropical Cyclone Landfall Processes (IWTCLP-III)*, Jeju, 8-10 Dec 2014.

Lee, C.S., L.R. Huang, H.S. Shen & S.T. Wang, 2006: A climatology model for forecasting typhoon rainfall in Taiwan, *Natural Hazards*, 37, 87-105.

Li, Xinfeng et al., 2013: Short-term forecasting of super typhoon Megi at landfall through cycling assimilation of China coastal radar data. *Journal of the Meteorological Sciences*. (in Chinese).

Lonfat, M., R. Rogers, T. Marchok & F. D. Marks Jr., 2007: A parametric model for predicting hurricane rainfall, *Mon. Wea. Rev.,* 135**,** 3086–3097.

Mannan Md. Abdul & Arjumand Habib, 2014: Understanding the properties of CS Aila using NWP technique. *Monitoring and Prediction of Tropical Cyclones in the Indian Ocean and Climate Change*, Ed. UC Mohanty, M Mohapatra, OP Singh, BK Bandyopadhyay and LS Rathore, pp 374-384.

Minakshi Devi et. al, 2013: Model prediction of cyclonic tracks over Bay of Bengal and resultant precipitation in the north-east region, Geomatics, *Natural Hazards and Risk* 04/2013.

Mitra, A.K., A.K. Bohra, M. Rajeevan & T. N Krishnalmurti, 2009: Daily Indian Precipitation Analysis Formed from a Merge of Rain-Guage Data with TRMM TMPA Satellite Derived Rainfall Estimates", *J. Meteor. Soc. Japan*, Vol. 87 A, pp 265-279.

Mohapatra, M., D.C. Gupta, N.K. Chinchlani & S.K. Dstidar, 2002: Orissa Super Cyclone, 1999 – a case study, *Journal of Indian Geophysical Union*, 6, 93-106.

Mohapatra, M., D.R. Sikka, B.K. Bandyopadhyay & Ajit Tyagi, 2013: Outcomes and challenges of Forecast Demonstration Project (FDP) over the Bay of Bengal, *Mausam* 64, 1 pp 1-12.

Nagata, K., 2010: Quantitative Precipitation Estimation and Quantitative Precipitation Forecasting by the Japan Meteorological Agency, *Technical Review, RSMC Tokyo-Typhoon Center*.

NHC, 2011: Tropical Cyclone Report: Hurricane Irene (AL092011), 21-28 August 2011. http://www.nhc.noaa.gov/data/tcr/AL092011_Irene.pdf

NWS, 2011: Service Assessment, Hurricane Irene, August 21-30, 2011. http://www.nws.noaa.gov/om/assessments/pdfs/Irene2012.pdf

Osuri, Krishna K. U. C. Mohanty, A. Routray & M. Mohapatra, 2012: The impact of satellite-derived wind data assimilation on track, intensity and structure of tropical cyclones over the North Indian Ocean, *Int. J. Remote Sens.*, 33, 5.

Pai D.S., Latha Sridhar, M. Rajeevan, O. P. Sreejith, N. S. Satbhai & B. Mukhopadhyay, 2014: Development of a new high spatial resolution (0.25° × 0.25°) long period (1901-2010) daily gridded rainfall data set over India and its comparison with existing data sets over the region", *Mausam*, 65, 1, 1-18.

Qi, L.B. & X.G. Cao, 2013: Analysis and comparison of forecasting of a heavy rainfall event in Shanghai under twin typhoons situation. *Journal of Tropical Meteorology.* (in Chinese)

Ray, K., M. Mohapatra, K. Chakravarthy, S. S. Ray, S.K. Singh & B. K. Bandopadhyay, 2014: Hydro-meteorological aspects of Tropical Cyclone Phailin in Bay of Bengal in 2013, *3rd International Workshop on Tropical Cyclone Landfall Processes (IWTCLP-III)*, Jeju, 8-10 Dec 2014.

Raju P. V. S. et al, 2012: Prediction of severe tropical cyclones over the Bay of Bengal during 2007–2010 using high-resolution mesoscale model, *Natural Hazards*, 01/2012.

Rappaport, E.N., 2000: Loss of Life in the United States Associated with Recent Atlantic Tropical Cyclones, *Bull. Amer. Meteor. Soc.*, 81, 2065–2073.

Routray, A., U.C. Mohanty, Krishna K. Osuri & S. Kiran Prasad, 2013: Improvement of Monsoon Depressions Forecast with Assimilation of Indian DWR Data Using WRF-3DVAR Analysis System, *Pure Appl. Geophys.*, 02/2013. doi: 10.1007/s00024-013-0648-z.

Satya, P., C. Mahesh, R.M. Gairola & P.K. Pal, 2012: Comparison of high-resolution TRMM-based precipitation products during tropical cyclones in the North Indian Ocean, *Natural Hazards* 12/2012; 61(2):689-701.

Scoccimarro, E., G. Villarini, S. Gualdi & A. Navarra, 2014: Changes in the precipitation associated to landfalling Tropical Cyclones in response to a warmer climate and increased CO_2, *3rd International Workshop on Tropical Cyclone Landfall Processes (IWTCLP-III)*, Jeju, 8-10 Dec 2014.

Singh, C., Sunit Das, R.B. Verma, B.L. Verma & B.K. Bandyopadhyay, 2012: Rainfall estimation of landfalling tropical cyclones over Indian coasts through satellite imagery, *Mausam*, 63, pp 193-202.

Sloughter, J.M, A.E. Raftery, T. Gneiting & C. Fraley, 2007: Probabilistic Quantitative Precipitation Forecasting Using Bayesian Model Averaging, *Mon. Wea. Rev.*, 135, 3209 – 3220

Srivastava K., 2014: Analysis and very short range forecast of cyclone 'AILA' with radar data assimilation with rapid intermittent cycle using ARPS 3DVAR and cloud analysis techniques", *Meteor. Atmos. Phys.*, 01/2014

Srivastava K., Rashmi Bhardwaj & S.K. Roy Bhowmik, 2011: Assimilation of Indian Doppler Weather Radar observations for simulation of mesoscale features of a land-falling cyclone, *Natural Hazards*, 01/2011

Srivastava, K., 2010: Analysis and very short range forecast of cyclone "AILA" with radar data assimilation with rapid intermittent cycle using ARPS 3DVAR and cloud analysis technique, *Atmosfera,* 01/2010.

Tallapragada, V., Chanh Kieu, Young Kwon, Samuel Trahan, Qingfu Liu, Zhan Zhang & In-Hyuk Kwon, 2013: Evalaution of Storm Structure from the Operational HWRF Model during 2012 Implementation, *Mon. Wea. Rev.*. doi:10.1175/MWR-D-13-00010.1

Tuleya, R.E., M. DeMaria & R.J. Kuligowski, 2007: Evalution of GFDL and simple statistical model rainfall forecasts for U.S. landfalling tropical storms, *Weather Forecasting*, 22, 56-69.

UKMO, 2014: Tropical Cyclones, http://www.metoffice.gov.uk/weather/tropicalcyclone

Van Nguyen, H. & Y. L. Chen, 2011: High-Resolution Initialization and Simulations of Typhoon Morakot (2009). *Mon. Wea. Rev.*, 139, 1463–1491.

Villarini, G., R. Goska, J.A. Smith & G.A. Vecchi, in press: North Atlantic tropical cyclones and U.S. flooding. *Bull. Amer. Meteor. Soc.*.

Weng, Y., F. Zhang, 2012: Assimilating Airborne Doppler Radar Observations with an Ensemble Kalman Filter for Convection-Permitting Hurricane Initialization and Prediction: Katrina (2005). *Mon. Wea. Rev.,* 140, 841–859

Woo, W. C., 2013a: Location-Based Rainfall Nowcasting Service for Public. *European Geosciences Union General Assembly 2013*, Vienna, Austria.

Woo, W. C., 2013b: Enhancement of optical flow technique for Nowcasting of springtime squall lines over Hong Kong. *The Fifth International Workshop on Monsoons*.

Woo, W. C., 2013c: Rain forecast on MyObservatory - a location-based rainfall nowcasting service for the public. *The 14th Workshop on meteorological operational systems*, ECMWF, Reading, U.K..

Woo, W. C., K. K. Li & Michael Bala: . An Algorithm to Enhance Nowcast of Rainfall Brought by Tropical Cyclones Through Separation of Motions. *Tropical Cyclone Research and Review*, 2014, 3(2): 111-121.

Yeung, H.Y., C. Man, S.T. Chan & A. Seed, 2014: Development of an operational rainfall data quality-control scheme based on radar-raingauge co-kriging analysis. *Hydrological Sciences Journal*, 59 (7), 1285–1299. doi:10.1080/02626667.2013.839873

Yu, Zifeng et al., 2014: Overview of Severe Typhoon Fitow and Its Operational Forecasts. *Tropical Cyclone Research and Review. http://www.hfip.org/documents/hfip_strategic_plan_yrs5-10_2013.pdf*

Yue, C., Y. Shou, S. Shou, G. Zeng & Y. Wang, 2007: Wet Q vector interpretation technique technique with its application to quantitative precipitation forecast, *Journal of Applied Meteorological Science*, 18, 666-675 (in Chinese)

Zhang, M., M. Zupanski, M. J. Kim & J.A. Knaff, 2013: Assimilating AMSU-A Radiances in the TC Core Area with NOAA Operational HWRF (2011) and a Hybrid Data Assimilation System: Danielle (2010). *Mon. Wea. Rev.*, 141, 3889–3907.

Zhong, Y., H. Yu, W. Teng & P. Chen, 2009: A dynamic similitude scheme for tropical cyclone precipitation forecast, *Journal of Applied Meteorological Science*, 20, 17-27 (in Chinese)